

# Combined Numerical and Experimental Investigation of a Centrifugal Compressor with Surge Suppression Holes at the Impeller Hub

**Zsolt Faltin, Károly Beneda**

Budapest University of Technology and Economics, Faculty of Transportation Engineering and Vehicle Engineering, Department of Aeronautics and Naval Architecture, Műegyetem rkp. 3, 1111 Budapest, Hungary  
faltin.zsolt@kjk.bme.hu; beneda.karoly@kjk.bme.hu

---

*Abstract: Centrifugal compressor surge is a very dangerous phenomenon to the working environment of a compression system. Unfortunately, the most efficient working range is close to the boundary of stable operation and surge situation. One of the main aims of this research project is to find a solution which can help to operate centrifugal compressor close to the instabilities with a much higher level of safety. A numerical investigation was made to examine the flow field and the centrifugal compressor behaviour at the onset of surge conditions both when compressor discharge bleed air was set and when the bleed air valve was closed. With the help of the numerical investigation, the calculation of the flow field was calculated in every compressor impeller blade passage. In this way the development and the behavior of the injected bleed air to the main flow field in the impeller blade passages could be analyzed. The results of the numerical investigation was validated later with a test bench with the exact geometry of the numerical investigation.*

*Keywords: centrifugal compressor surge; compressor instabilities; bleed air; self recirculating air*

---

## 1 Introducing of Surge Suppression Techniques

Centrifugal compressor instabilities appear when the compressor has to work against much higher load pressure than it could overcome. These instabilities start with weak backflow near the wall of the compressor casing and later the increased backpressure causes rotating stall at the tip region of the impeller blades [1]. We can measure this rotating stall with high frequency and small amplitude pressure oscillations [2]. If the backpressure rises towards a critical point the pressure ratio suddenly drops to much lower level and the plenum starts to oscillate much higher amplitude and with lower frequency [3] [4]. We call this phenomenon Compressor Surge [5]. There are still a lot of existing techniques which can handle this

phenomenon very effectively [6], [7]. These solutions need a lot of energy to operate and sometimes for example with aviation engines the usage of these solutions results in power loss or needs heavy additional external equipment [8], which is not favorable in critical aerial situations.

The introduced novel method we have investigated in this work promises such a solution which does not need high energy consumption and a lot of added structural equipment.

## 2 Preliminary Elementary Investigation of the Surge Suppression Holes

Based on the earlier elementary results of this research [9] the injected flow from the impeller hub deflects the main flow in the impeller passages towards the outer section of the impeller which can increase the total pressure rise of the compression system based on the Euler head equation.

The basic model of the compressor characteristic [9]:

$$\Psi_c = \Psi_{c0} + H \left[ 1 + \frac{3}{2} \left( \frac{\varphi_c}{W} - 1 \right) - \frac{1}{2} \left( \frac{\varphi_c}{W} - 1 \right)^3 \right] \quad (1)$$

The basic equation completed with the model of the bleed air inflow:

$$\Psi_c(\varphi_c, \gamma_{BLDC}) = \Psi_{c0}(\gamma_{BLDC}) + H(\gamma_{BLDC}) \left[ 1 + \frac{3}{2} \left( \frac{\varphi_c}{W(\gamma_{BLDC})} - 1 \right) - \frac{1}{2} \left( \frac{\varphi_c}{W(\gamma_{BLDC})} - 1 \right)^3 \right] \quad (2)$$

where the meaning of the equation are:

$$\Psi_{c0}(\gamma_{BLDC}) = -6.25\gamma_{BLDC}^2 + 0.453\gamma_{BLDC} + 1.20 \quad (3)$$

$$H(\gamma_{BLDC}) = -5.00\gamma_{BLDC}^2 + 0.280\gamma_{BLDC} + 8.11 \cdot 10^{-2} \quad (4)$$

$$W(\gamma_{BLDC}) = -0.160\gamma_{BLDC} + 0.15 \quad (5)$$

With the completed mathematical model the calculation of the modified compressor characteristic will be:

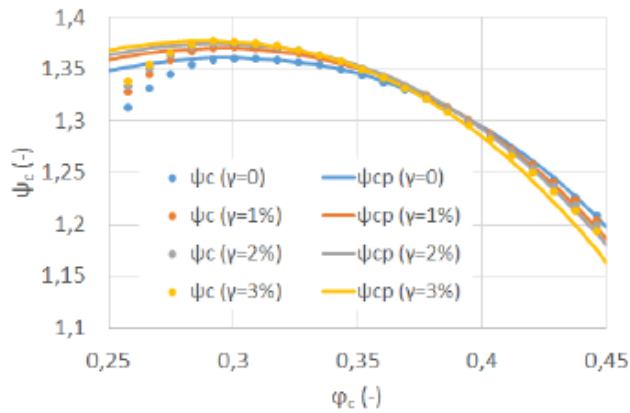


Figure 1

The result of the calculations with the modified compressor characteristic model [9]

Table 1

The essential values of the modified compressor characteristic model [9]

$\gamma_{BLDC}$ (%)	$\psi_{c0}$ (-)	H (-)	W (-)
0	1,199	0,081	0,015
1	1,203	0,0835	0,0148
2	1,2055	0,0845	0,0147
3	1,207	0,085	0,0145

This equation of the compressor characteristic will be then transformed to that implicit form where it will be the function of the  $\varphi$  and  $\gamma_{BLDC}$ .

$$\psi_c(\varphi_c, \gamma_{BLDC}) = \psi_{c0}(\gamma_{BLDC}) + H(\gamma_{BLDC}) + \frac{3}{2} \left( \frac{\varphi_c}{W(\gamma_{BLDC})} - 1 \right) H(\gamma_{BLDC}) - \frac{1}{2} \left( \frac{\varphi_c}{W(\gamma_{BLDC})} - 1 \right)^3 H(\gamma_{BLDC}) \quad (6)$$

Expanding the bracket at the second part of the equation:

$$\psi_c(\varphi_c, \gamma_{BLDC}) = \psi_{c0}(\gamma_{BLDC}) + H(\gamma_{BLDC}) + \frac{3}{2} \frac{H(\gamma_{BLDC})}{W(\gamma_{BLDC})} \varphi_c - \frac{3}{2} H(\gamma_{BLDC}) - \frac{1}{2} \left( \frac{\varphi_c}{W(\gamma_{BLDC})} - 1 \right)^3 H(\gamma_{BLDC}) \quad (7)$$

And after doing the same transformation at the third member of this equation:

$$\begin{aligned}
\left(\frac{\varphi_c}{W(\gamma_{BLDC})} - 1\right)^3 &= \left(\frac{\varphi_c}{W(\gamma_{BLDC})} - 1\right)\left(\frac{\varphi_c}{W(\gamma_{BLDC})} - 1\right)\left(\frac{\varphi_c}{W(\gamma_{BLDC})} - 1\right) \\
&= \left[\left(\frac{\varphi_c}{W(\gamma_{BLDC})}\right)^2 - 2\frac{\varphi_c}{W(\gamma_{BLDC})} + 1\right]\left(\frac{\varphi_c}{W(\gamma_{BLDC})} - 1\right) = \\
&= \left(\frac{\varphi_c}{W(\gamma_{BLDC})}\right)^3 - 2\left(\frac{\varphi_c}{W(\gamma_{BLDC})}\right)^2 + \frac{\varphi_c}{W(\gamma_{BLDC})} - \left(\frac{\varphi_c}{W(\gamma_{BLDC})}\right)^2 + \\
&= 2\frac{\varphi_c}{W(\gamma_{BLDC})} - 1 = \left(\frac{\varphi_c}{W(\gamma_{BLDC})}\right)^3 - 3\left(\frac{\varphi_c}{W(\gamma_{BLDC})}\right)^2 + 3\frac{\varphi_c}{W(\gamma_{BLDC})} - 1
\end{aligned} \tag{8}$$

And the final form will be:

$$\begin{aligned}
\Psi_c(\varphi_c, \gamma_{BLDC}) &= \Psi_{c0}(\gamma_{BLDC}) + H(\gamma_{BLDC}) + \frac{3}{2} \frac{H(\gamma_{BLDC})}{W(\gamma_{BLDC})} \varphi_c - \\
&= \frac{3}{2} H(\gamma_{BLDC}) - \frac{1}{2} \left[ \left(\frac{\varphi_c}{W(\gamma_{BLDC})}\right)^3 - 3\left(\frac{\varphi_c}{W(\gamma_{BLDC})}\right)^2 + 3\frac{\varphi_c}{W(\gamma_{BLDC})} - 1 \right] H(\gamma_{BLDC})
\end{aligned} \tag{9}$$

After some simplification:

$$\begin{aligned}
\Psi_c(\varphi_c, \gamma_{BLDC}) &= \Psi_{c0}(\gamma_{BLDC}) - \frac{1}{2} H(\gamma_{BLDC}) + \frac{3}{2} \frac{H(\gamma_{BLDC})}{W(\gamma_{BLDC})} \varphi_c - \\
&= \frac{1}{2} \frac{H(\gamma_{BLDC})}{W^3(\gamma_{BLDC})} \varphi_c^3 + \frac{3}{2} \frac{H(\gamma_{BLDC})}{W^2(\gamma_{BLDC})} \varphi_c^2 - \frac{3}{2} \frac{H(\gamma_{BLDC})}{W(\gamma_{BLDC})} \varphi_c + \frac{1}{2} H(\gamma_{BLDC})
\end{aligned} \tag{10}$$

We can simplify this equation with residual members of the  $H(\gamma_{BLDC})$  and with the  $\frac{3}{2} \frac{H(\gamma_{BLDC})}{W(\gamma_{BLDC})} \varphi_c$  the final form of the modified equation of the characteristic will look like:

$$\Psi_c(\varphi_c, \gamma_{BLDC}) = \Psi_{c0}(\gamma_{BLDC}) - \frac{1}{2} \frac{H(\gamma_{BLDC})}{W^3(\gamma_{BLDC})} \varphi_c^3 + \frac{3}{2} \frac{H(\gamma_{BLDC})}{W^2(\gamma_{BLDC})} \varphi_c^2 \tag{11}$$

This means that this flow injection increases the total energy of the fluid goes through the impeller. Further advantage of this method is that in certain circumstances this flow injection can stabilize the operation of the centrifugal compressor at the onset of surge situation. [9]

### 3 Integration of the Modified Impellers into the Original Turbocharger

The experimental impellers were made with one of the fast prototype manufacturing processes by polyamid material with SLS (selective laser sintering) technology at Varinex Ltd. The base 3D model of the original impeller was made by CATIA V5 design environment.

The base modification of the original impeller design was to create the holes in the impeller hub section to realize the air backflow from volute section. It could be seen below some pictures about the 3D printed model. To prevent the flow to escape from the previously mentioned central interface section between the impeller hub and volute labyrinth sealing was created with also positive and negative shaping to overlap the opposite faces. It was proven that this labyrinth sealing was effective because the smutty signs of the radial flow had disappeared by the usage of this type of sealing. The calculation of the boundary layer.

Length scale of the flow:  $L=0,09$  m

Dynamic viscosity of air:

$$\mu = 19,4 \cdot 10^{-6} \frac{\text{kg}}{\text{m} \cdot \text{s}}$$

Density of the ambient air:

$$\rho = \frac{P}{R \cdot T} = \frac{140000}{287 \cdot 315} = 1,54 \frac{\text{kg}}{\text{m}^3}$$

Kinematic viscosity of air:

$$\nu = \frac{\mu}{\rho} = \frac{19,4 \cdot 10^{-6}}{1,54} = 1,2597 \cdot 10^{-5} \frac{\text{m}^2}{\text{s}}$$

The Reynolds-number:

$$\text{Re} = \frac{V \cdot L}{\nu} = \frac{50 \cdot 0,09}{1,2597 \cdot 10^{-5}} = 357227,9157$$

Shear stress velocity at the wall:

$$U_{\tau} = \sqrt{\frac{\tau_w}{\rho}} = \sqrt{\frac{8,655}{1,54}} = 2,37 \frac{\text{m}}{\text{s}}$$

Wall shear stress:

$$\tau_w = \frac{1}{2} \cdot C_f \cdot \rho \cdot V^2 = \frac{1}{2} \cdot 0,004496 \cdot 1,54 \cdot 50^2 = 8,655 \frac{\text{kg}}{\text{m} \cdot \text{s}^2}$$

The skin friction on a plate:

$$C_f = 0,058 \cdot \text{Re}^{-0,2} = 0,058 \cdot 357227,9157^{-0,2} = 0,004496$$

The first cell height from the wall:

$$y = \frac{y^+ \cdot \nu}{U_\tau} = \frac{1 \cdot 1,2597 \cdot 10^{-5}}{2,37} = 5,315 \cdot 10^{-6} \text{ m} = 0,005315 \text{ mm}$$

The boundary layer thickness:

$$\delta = 0,035 \cdot L \cdot \text{Re}^{-\frac{1}{7}} = 0,035 \cdot 0,09 \cdot 357227,9157^{-\frac{1}{7}} = 0,507 \text{ mm}$$

The calculation of the Knudsen-number criterion:

The mean free path of the molecules:

$$\lambda = \frac{R \cdot T}{\sqrt{2} \cdot \pi \cdot d_a^2 \cdot A \cdot P} = \frac{8,3145 \cdot 315}{\sqrt{2} \cdot \pi \cdot (3,57 \cdot 10^{-10})^2 \cdot 6 \cdot 10^{23} \cdot 140000} = 5,5065 \cdot 10^{-8} \text{ m}$$

The gas constant:

$$R = 8,3145 \frac{\text{J}}{\text{mol} \cdot \text{K}}$$

Total temperature at the OUTLET: T=315K

Total pressure at the OUTLET: 140000Pa

Molecule's average diameter:

$$d_a = 3,57 \cdot 10^{-10} \text{ m}$$

Avogadro's number:

$$A = 6 \cdot 10^{23} \frac{1}{\text{mol}}$$

The Knudsen-number:

$$\text{Kn} = \frac{\lambda}{L} = \frac{5,5065 \cdot 10^{-8}}{0,001} = 0,00005065 < 0,01$$

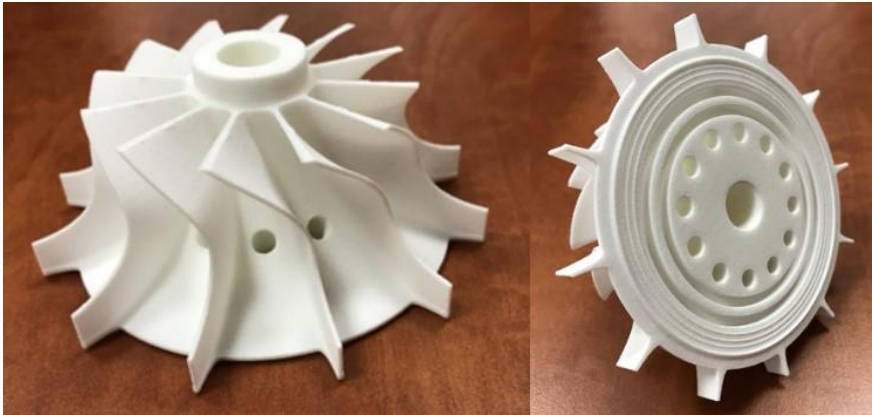


Figure 2

The 3D printed impeller with the recirculation holes in the imeller hub

The 3D printed model was easy to access the original shaft of the Holset turbocharger because it was sized to strictly adjust with the baseline hole. The backflow originates from the centrifugal compressor volute section through a drain hole which ends at the backplate of the compressor volute in a flat cylinder at a diameter of the impeller holes on the backplate of the impeller hub section. As it could be seen on Figure 2, labyrinth sealing was designed to prevent the escape of the high pressure backflow between the backplate of the impeller and aft wall of the diffuser casing. During the test runs these sealing have proved that they can hold the pressure inside the hub of the impeller.

## 4 Numerical Studies about Centrifugal Compressor Surge

In parallel with development of the computers the calculation capacities of processors multiplied every year. In this way more and more detailed numerical investigations could be realized as in Lu et al. [10], especially in the technologies of turbomachinery and also numerous turbulence models could be used to calculate unsteady flows, e.g. in Jiang et al. [11], for example the Large Eddy Simulation from Zhang et al. [12] or the Reynolds-averaged Navier-Stokes with Shear Stress Transport model in Hu et al. [13]. There are a lot of different types of numerical softvers and some of them are able to calculate *transient* phenomenons like centrifugal compressor surge. For solving the flow governing equations the ANSYS CFX numerical solver was used and the SST model for calculating the turbulences because it combines the advantages of the  $k-\varepsilon$  and the  $k-\omega$  models. There are still a lot of attempts to increase the stable operating range of centrifugal

compressors, for example Halawa *et al.* [14], or Siyue *et al.* [15]. Here, will be examined a method which uses flow injection from the impeller hub.

## 5 Prelude Studies of the Numerical Investigation

In the past years elementary investigation was made to examine the injected bleed air perpendicular to the main flow in the compressor blade passages. In the prelude article of Beneda and Faltin [16] a mathematical model was developed to calculate the total pressure rise comes from the usage of bleed air in the centrifugal compressor characteristic map. Air injection is a widely examined method to stabilize compressor operation, one of them is presented in Li *et al.* [17] As the model predicted if the 5-7 percent of the total mass flow rate is used as bleed air injected from the compressor impeller hub section, the total pressure developed by the compressor system at the discharge section could be increased by 2-3%. A stress assessment was made by Beneda and Faltin [18] to calculate the effect of these holes to the mechanical behaviour of the impeller.

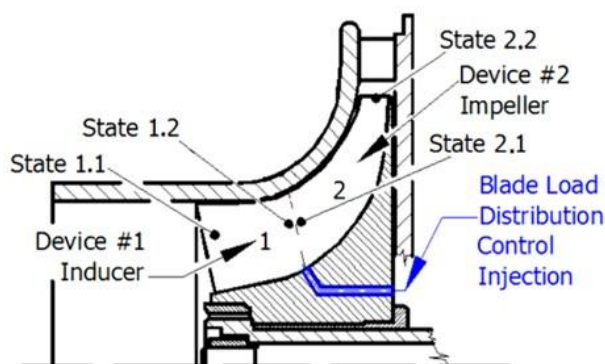


Figure 3

The position of the recirculating slots in the impeller hub [16]

But this mathematical model considered ideal circumstances, so further investigations were needed to discover the effects of the injected bleed air to the compression system. Before developing a real test bench to validate the elementary considerations numerical investigation was made by the method of computational fluid dynamics, in short CFD.

## 6 Settings of the Numerical Investigation

The basic elements of the 3D model for the CFD simulation comes from the complete turbocharger section of the engine of a Diesel-electric locomotive. After the complete disassembly of the compressor stage of this turbocharger, all of the necessary geometries were created in CATIA V5 design environment to create the compression system for numerical investigation. This model included the compressor impeller with the casing, the fix bladed diffuser and the constant cross-sectional volute. After the volute outlet area, at the discharge section the 3D model of the choke throttle valve was also created, basically it is a butterfly valve. Besides the control of the rotational periodicity of the turbocharger, this throttle valve was mainly responsible for setting the onset of surge condition during real measurements on the test bench. In case of the inlet section of the compressor only the confusor shaped air intake section was made with the extension of the inlet circular geometry by duplication of its length.

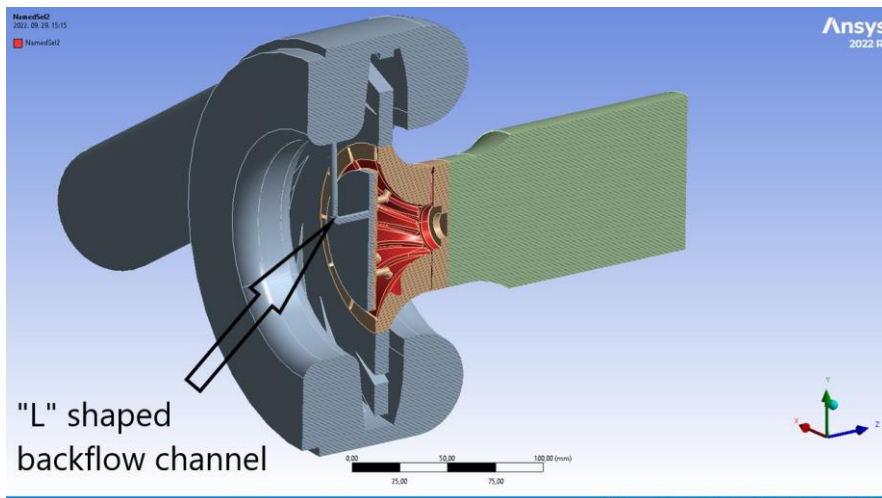


Figure 4

The vertical cross-sectional view of the flow field of the compressor and the recirculating slots

Because of the main goal of the simulation is to investigate highly transient phenomenon in the centrifugal compressor it is obvious that the flow direction of the fluid can be opposite than the normal flow direction. From this consideration in the model the inlet and the outlet cross-section were set to Opening type. This means that for discretization of the problem it was necessary to define the inlet and the outlet parameters of the working fluid, but because of the complete 3D geometry of the examined compression system was made, it was enough to define the ambient characteristics of the air at the inlet and the outlet section. The Shear Stress Transport model was used to calculate the flow near the wall so at the

critical parts of the wall, for example at the inner casing section at the impeller blade tips, at the diffuser passages and at the butterfly valve, the element size was reduced from 0,5 mm to 0,1 mm and Inflation settings with Growth rate of 1,2. The  $y^+$  parameter occurs in between the values of 30 and 300. It was checked by the Isovolume function and by reducing the element sizes, the grid independency was checked in 5 steps. The number of nodes are 4266577 and the number of elements are 13336470.

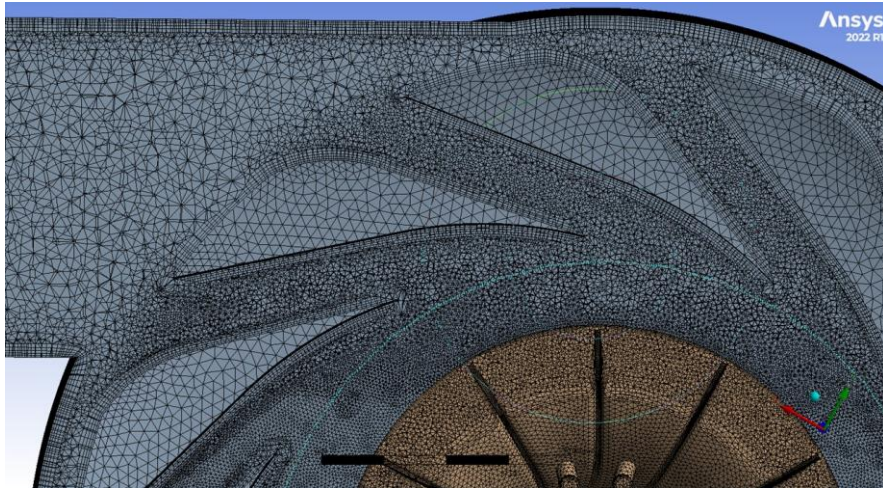


Figure 5

Grid distributions at the critical parts of the geometry on aft view

In the later performed transient runnings this assumption proved very useful and effective. The real characteristic of the experimental centrifugal compressor was made for the entire working range from 20,000 to 40,000 RPM with the settings of the throttle valve from full open position to the fully closed position.

The stable and the unstable working areas of the compressor could be clearly measured. During the numerical investigation amongst the ambient parameters only the angle of attack of the throttle valve and the rotational periodicity of the impeller were set and the results were checked by the calculated mass flow rate at the inlet section of the model and the calculated pressure rise at the cylinder shaped section between the compressor discharge and the butterfly type throttle valve. The difference between the results of the numerical calculation and the real measurements were less than 1 percent, the total mass flow rate was calculated with thousandths in accuracy. In this way the model was able to examine the effects of the injected bleed air from the impeller hub section of the compressor.

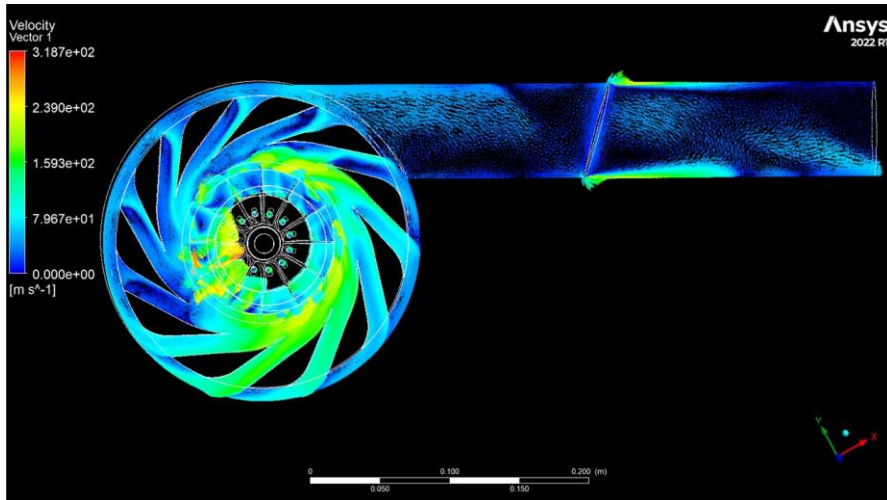


Figure 6

Front view of the compressor while transient simulation was set

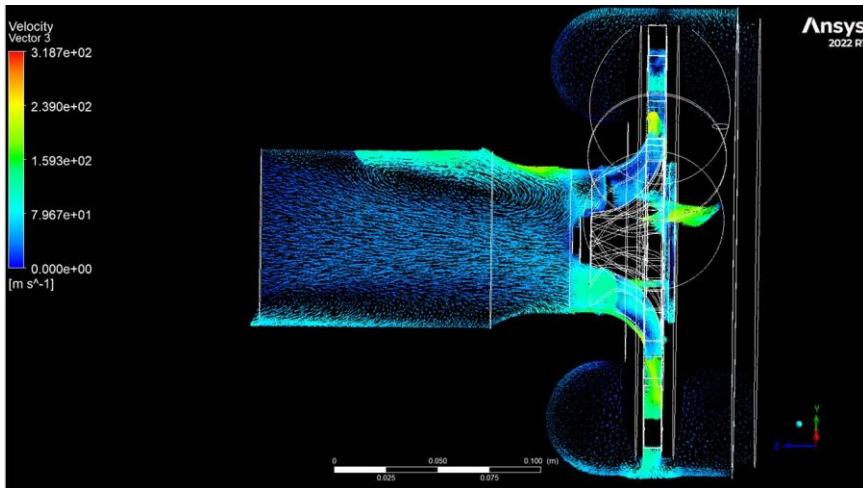


Figure 7

Side view of the compressor while backflow occurs at the inlet section

## 7 Steady State Examinations

After the validation of the 3D model, the bleed air holes were created in the model in accordance with the earlier elementary investigations. During the numerical simulations different impeller designs were examined with air bleed holes with 2 to 4 mm in diameter. The numerical examinations have resulted that the design with 4 mm holes caused considerable pressure rise at the discharge area of the compressor, so the results of the numerical calculations have proved the results of the elementary mathematical model. The following table contains the calculated results at different rotational speeds.

Table 2

The results of the Steady State calculation at different RPMs and Bleed valve positions

RPM	Valve Off/On	$\Delta p_2$ [Pa]	$T_2$ [K]	$\dot{m}$ [kg/s]	$\eta_{sc}$ [-]
60000	0	69304,5	416,228	0,4409	0,419003
60000	1	69745,2	422,933	0,4481	0,398258
70000	0	72682,9	387,586	0,5315	0,578561
70000	1	72943,1	393,529	0,5388	0,543412
80000	0	961985	454,071	0,5685	0,413452
80000	1	970903	461,082	0,5752	0,398384
85000	0	103310	475,131	0,5853	0,384966
85000	1	104400	482,958	0,58816	0,371567
90000	0	118852	455,06	0,5932	0,485193
90000	1	119597	464,611	0,61042	0,459256

These calculations were performed in the stable operational range of the centrifugal compressor. In this way it was enough to use *Steady State* calculation formulas to prove the acceptable results. As it could be seen on the table the usage of bleed air injected into the blade passages could increase the overall pressure rise of the compression system, but total temperature rise with considerable amount was associated to this advantage of pressure rise which means that in total isentropic efficiency loss was measured.

## 8 Transient Examinations

The investigation of the bleed air holes was continued to the unstable operating range of the centrifugal compressor. This mode of operation shows very transient behaviour, so to perform this numerical calculations in the ANSYS, *Transient* module was used. To accomplish transient runnings in ANSYS at first the initial parameters have to be defined. This parameter initialization comes from the

results of the steady state examinations. During transient phenomena the parameters observed by the solver, for example the imbalance, could not converge to an exact value, but also it starts to oscillate. To take into account the time dependent behaviour of the flow the transient term could be used. In this term the time dependent equations are discretized and for solving these equations additional initial parameters are needed. For the conservation equations the initial values could be described from the result of an earlier steady state calculation and because of the discretization of the time dependent governing equations, total time duration and for the interval time steps have to be defined. Because of the high resolution nature of the surge phenomenon in this case 1ms was set for the Time Step variable and 3s for the Total Time. The results have shown that when the surge phenomenon occurs total pressure drop and total temperature rise were calculated at the discharge section of the centrifugal compressor. These results were later confirmed by real measurements.

## 9 Results of the Investigation

The turbocharger was operated at a lot of different RPM levels with the maximum value of 40.000. The throttle valve of the compressor could be operated both automatically by the digital measurement and control system and manually to adjust its position appropriately to the onset of surge condition of the compressor. The BLDC valve could be operated only manually, but it has a position indicator and its operation can be saved by the digital measurement system. When the mode of the compressor was set to the onset of surge condition, the throttle valve was fixed by a butterfly screw and the BLDC valve was operated open and closed position from 5 to 10 seconds multiple times. When the BLDC valve was opened the backflow goes through the impeller holes from the volute section to the impeller channels and as it could be seen on the diagrams below, with the help of this backflow the stabilized operational mode of the centrifugal compressor could be regained multiple times. Additionally, it is also absolutely visible on the diagram that the main flow in the compressor destabilized into surge condition when the backflow from the volute section was stopped by closing the BLDC valve. This measurement was repeated two weeks later with an other 3D printed impeller with same geometry and the results were the same as at the first attempt. Afterward these measurements were repeated by modified centrifugal compressor impellers with increased diameter holes at the impeller hub.

A numerical simulation was also made to discover the effects of the operation of the backflow valve and the flow regime inside the centrifugal compressor and inside its blade passages. The figure below shows that this backflow compelled the main flow to the upper part of the blade passages and accelerates it also, which results in higher total energy of the fluid.

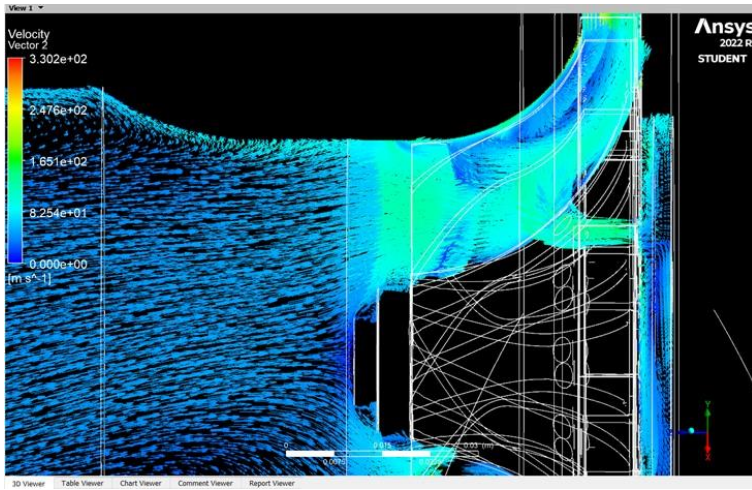


Figure 8

Numerical simulation of the backflow through the impeller hub

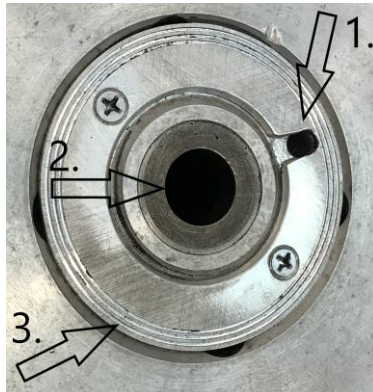


Figure 9

The outer section of the BLDC backflow channel (marked by 1.) can be seen on Figure 9 and the opposite side of the labyrinth sealing (marked by 3.) placed on the front wall of the centrifugal compressor volute section. The plain bearings of the compressor shaft is shown by 2.

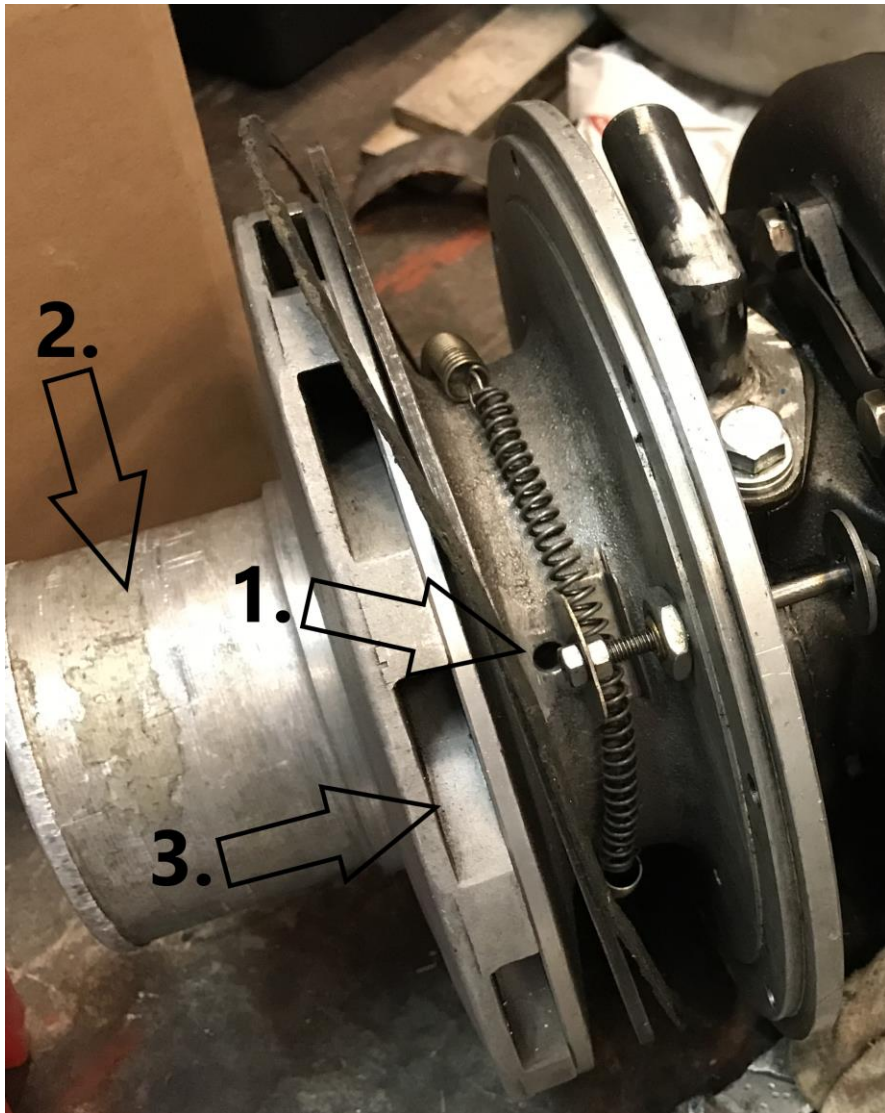


Figure 10

The structure of the BLDC valve can be seen on the Figure 9. An “L” shape hole was created on the inner section of the centrifugal compressor volute section. This is marked by 1. A metal plate was used to overlap this hole when the backflow was stopped. This metal plate was strengthened to the inner volute wall with a circumferential spring. The air comes from the inlet duct, marked 2. on the figure and comes from the diffuser outlet section, marked with 3. When the onset of surge occurs at 38.000RPM at closed BLDC valve, with the help of the screw rod attached to the plate the valve can be turned from closed to open position and the surge phenomenon stopped as it can be seen on Figure 10.

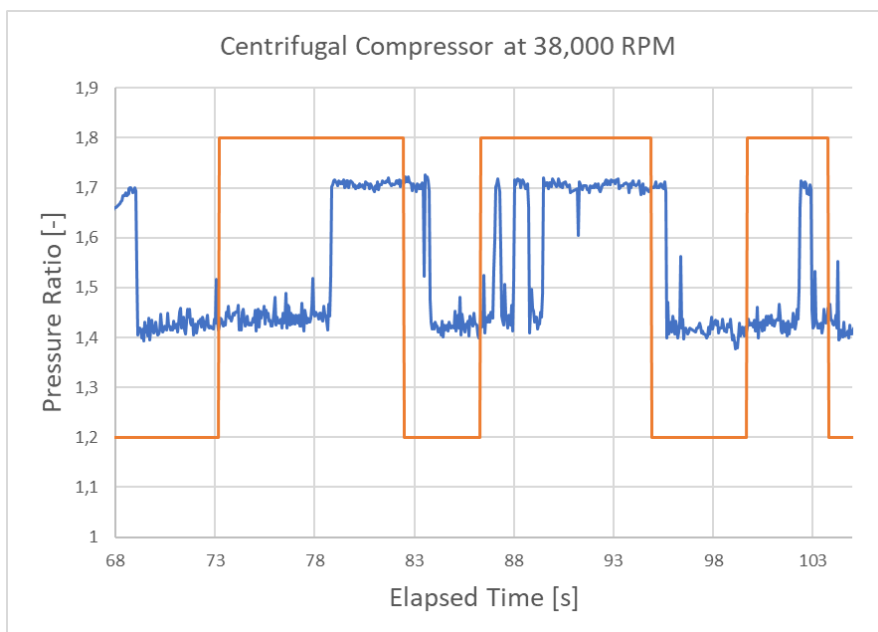


Figure 11

The measured compressor discharge pressure during the operation of the backflow valve

As it can be seen on the diagrams the onset of surge condition was set by a throttle valve at the discharge section of the compressor at a constant speed of 38,000 RPM. By continuously closing the throttle valve at the point of the onset of surge the total pressure drop could be seen. The pressure sensors indicate that the pressure oscillates in the system and it can be observed that in certain condition when the BLDC valve was opened the pressure oscillation had been stopped and the measured total pressure at the discharge section returned to the nominal value of the stable operation. Closing the BLDC valve caused the system falling back into surge condition.

## Conclusions

Based on the results we can declare that the backflow from the volute section to the impeller tunnels through the holes in the impeller section can handle the onset of surge condition of the centrifugal compressor and can stabilize the main flow in the impeller and the operation of the compressor with the regain of the total pressure at the compressor discharge and the mass flow rate of the main flow. In some case the reaction of the system was slow, it can be seen that sometimes it takes 3-5 seconds from the BLDC valve opening to regain the stabilized main flow in the compressor.

## References

- [1] E. M. Greitzer: Surge and Rotating Stall in Axial Flow Compressors, Part I. Theoretical Compression System Model. Transactions of the ASME, 1976
- [2] Jan Tommy Gravdahl and Olav Egeland: A Moore-Greitzer axial compressor model with spool dynamics. Proceedings of the 36<sup>th</sup> Conference on Decision & Control, San Diego, California USA, December, 1997 IEEE 0-7803-3970-8
- [3] Filip Grapow and Grzegorz Liskiewicz: Study of the Greitzer Model for Centrifugal Compressors: Variable  $L_c$  Parameter and Two Types of Surge. Energies 2020, 13, 6072; doi:10.3390/en13226072
- [4] Se Young Yoon, Zongli Lin, Chris Goyne and Paul E. Allaire: An Enhanced Greitzer Compressor Model with Pipeline Dynamics Included. 2011 American Control Conference on O'Farrell Street, San Francisco, CA, USA June 29-July 01, 2011 AACC 978-1-4577-0081-1/11
- [5] Beat Ribi, Georg Gyarmathy: Impeller Rotating Stall as a trigger for the transition from Mild to Deep Surge in a Subsonic Centrifugal Compressor. International Gas Turbine and Aeroengine Congress and Exposition, ASME, Cincinnati, Ohio – May 24-27, 1993
- [6] H. Mohtar, P. Chesse, and D. Chalet: Effect of a map width enhancement system on turbocharger centrifugal compressor performance and surge margin; Proc. IMechE Vol. 225, Part D: J. Automobile Engineering DOI: 10.1177/2041299110393191
- [7] Xu W, Wang T, Gu C G. Performance of a centrifugal compressor with holed casing treatment in the large flowrate condition. Sci China Tech Sci, 2011, 54: 2483-2492, doi: 10.1007/s11431-011-4416-y
- [8] Yuichiro Asaga, Shimpei Mizuki, Hoshio Tsujita and Shinsuke Ohta: Surge Control of a Centrifugal Compressor System by using a Bouncing Ball; Journal of Thermal Science Vol.17, No.2 (2008) 141-146, Article ID: 1003-2169(2008)02-0141-06, DOI: 10.1007/s11630-008-0141-7
- [9] Zsolt Faltin, Károly Beneda: Establishment of Meanline Compressor Mathematical Model with Active Blade load Distribution Control. 2020 IEEE 18<sup>th</sup> World Symposium on Applied Machine Intelligence and Informatics (SAMI), 23-25 January 2020, DOI:10.1109/SAMI48414.2020.9108751
- [10] Tianyu Lu, Xiaosheng Wu, Juanmian Lei, Jintao Yin: Numerical study on the aerodynamic coupling effects of spinning and coning motions for a finned vehicle. Aerospace Science and Technology 77 (2018) 399-408, <https://doi.org/10.1016/j.ast.2018.03.027>
- [11] Jiang S., Li Z., Li J., and Song L. (2023) Numerical investigations on the unsteady leakage flow and heat transfer characteristics of the turbine blade

- squealer tip. *Journal of the Global Power and Propulsion Society*. 7: 1-12, <https://doi.org/10.33737/jgpps/157176>
- [12] Yufei Zhang, Haixin Chen, Song Fu and Wenjiao Dong: Numerical study of an airfoil with riblets installed based on large eddy simulation. *Aerospace Science and Technology* 78 (2018) 661-670 <https://doi.org/10.1016/j.ast.2018.05.013> 1270-9638/ 2018 Elsevier Masson SAS
- [13] Jiaguo Hu, Qiushi Li, Tianyu Pan and Yifang Gong: Numerical investigations on stator hub initiated stall in a single-stage transonic axial compressor. *Aerospace Science and Technology* 80 (2018) 144-155, <https://doi.org/10.1016/j.ast.2018.07.018> 1270-9638/ 2018 Elsevier Masson SAS
- [14] Taher Halawa, Mohamed Alqaradawi, Mohamed S. Gadala, Ibrahim Shahin, Osama Badr: Numerical Investigation of Rotating Stall in Centrifugal Compressor with Vaned and Vaneless Diffuser. *Journal of Thermal Science* Vol. 24, No. 4 (2015) 323-333, Article ID: 1003-2169(2015)04-0323-11, DOI: 10.1007/s11630-015-0791-1
- [15] Chen Siyue, Zuo Shuguang, Wei Kaijun: Numerical Investigation of the Centrifugal Compressor Stability Improvement by Half Vaned Low Solidity Diffusers. *Journal of Thermal Science* Vol. 30, No. 2 (2021) 696-706, Article ID: 1003-2169(2021)02-0696-11, <https://doi.org/10.1007/s11630-021-1318-6>
- [16] Zsolt Faltin, Károly Beneda: Establishment of Meanline Compressor Mathematical Model with Active Blade load Distribution Control. 2020 IEEE 18<sup>th</sup> World Symposium on Applied Machine Intelligence and Informatics (SAMI), 23-25 January 2020, DOI:10.1109/SAMI48414.2020.9108751
- [17] Jichao Li, Juan Du, Chaoqun Nie and Hongwu Zhang: Review of tip air injection to improve stall margin in axial compressors. *Progress in Aerospace Sciences* 106 (2019) 15-31, <https://doi.org/10.1016/j.paerosci.2019.01.005>
- [18] Z. Faltin and K. Beneda, "Stress Assessment of Centrifugal Compressor with Surge Suppression Holes in the Impeller Hub," *2019 New Trends in Aviation Development (NTAD)*, Chlumec nad Cidlinou, Czech Republic, 2019, pp. 40-44, doi: 10.1109/NTAD.2019.8875526